

Changes in diffusion through the brain extracellular space

Manuel Mota*¹, José A. Teixeira*, José B. Keating[†] and Alexander Yelshin*

*Centro de Engenharia Biológica – Instituto de Biotecnologia e Química Fina, Universidade do Minho, Campus de Gualtar, 4710-057 Braga, Portugal, and [†]Faculdade de Medicina, Universidade de Coimbra, Rua Larga, 3049 Coimbra Codex, Portugal

ECS (extracellular space) works as the microenvironment of brain cells. Diffusion through ECS may be described through an effective diffusion coefficient, D_e , which in turn depends on ECS porosity, ε , and tortuosity, T . In the present research, diffusion data together with ε and T were collected from the specialized literature and analysed to seek a correlation of T versus ε . On the basis of D_e data, upper and lower T boundaries were defined and related to topologically 'dense' and 'loose' cell arrangement. A possible range for T variation was obtained for ECS, with ε ranging from 0.05 to 0.6. A tortuosity index (n) in the form of T and ε logarithmic ratio was introduced. This index may be adopted for recalculation of T or ε if only one of these parameters is known. As a result of data analysis and modelling, it was concluded that, upon different external conditions, for instance oxygen depletion, the ECS porosity decreases and cells (presumably through membrane rearrangements) adjust the void space to keep the diffusion within a defined range, which gives the living tissue the ability to maintain the diffusion level up to two or more times higher than in conventional granular bed packing. Thus, even with a dramatic ECS decrease, the cellular system is still able to support a given diffusion by decreasing the value of T . The obtained results clearly show the existence of three data clusters: a region of normal brain functioning, both for young and adult brains, for values of ε comprised between 0.15 and 0.30, and two regions of abnormal brain behaviour to the left and to the right of the normal region, corresponding to different states (aging, tumours, anoxia, brain death, etc.). The present approach allows defining the optimal range of ε and T to assure the best ECS diffusion efficiency for a specified macromolecule. This might be important in brain clinical treatment.

Introduction

Brain ECS (extracellular space) plays an important role in many processes related to brain activity. ECS occupies about 20% of nervous tissue volume and serves as the microenvironment of nerve cells. An example of ECS

geometry is shown, for instance, in [1]. Chemical species such as ions, metabolites, peptides, neurohormones and other neuroactive substances and molecules circulate in ECS. ECS directly or indirectly affects neuronal and glial cell functions and serves as an important communication channel [2–4].

Diffusion through ECS may be described through an effective diffusion coefficient, D_e , which in turn depends on ECS porosity or ECS volume fraction, ε , and on tortuosity T . Tortuosity may be defined as the ratio between the average pathway of a moving object, for instance, a diffusing molecule, to the minimal possible distance between the inlet and the outlet points of the diffusion medium [5–7].

Modelling diffusion through brain tissue is more complicated than the case of diffusion in porous media, for several reasons: (1) ECS has a rather complicated physical three-dimensional structure; (2) brain tissue responds dynamically to changes in environmental conditions; and (3) there is increasing evidence of selective segregation of large molecules that might exclude them from certain ECS regions. Finally, ECS and ε change drastically in several pathological states. The complicated structure of the ECS makes it difficult to build theoretical models for diffusion in this case.

A large set of experimental data on diffusion in ECS for different physiological conditions has been accumulated in the specialized literature and may serve to propose a generalized approach.

In the present research, brain diffusion data together with ε and T were collected and analysed in the form of a T -versus- ε correlation in order to compare them with the diffusion data of mineral materials where the dependence of the porosity on tortuosity may be defined by two parameters, one of which usually is assumed to be constant. Further on, an attempt to correlate the results obtained with several brain pathological states will be made in order

Key words: brain pathology, extracellular space, hindered macromolecule diffusion, porosity, tortuosity.

Abbreviations used: CW, cranial window; DC, dorsal chamber; ECS, extracellular space; HPMA, *N*-(2-hydroxypropyl)methacrylamide; TMA⁺, tetramethylammonium.

¹ To whom correspondence should be addressed (e-mail mmota@deb.uminho.pt).

to see whether those results might help define the kind of macromolecule suitable to deal with each pathological situation.

Theory

Diffusion and tortuosity

Tortuosity is usually obtained from diffusion experiments. Nicholson and Rice [8] confirmed that Ca^{2+} diffusion is mainly influenced by the tortuosity of the tissue rather than by other factors such as binding to extracellular charge sites or uptake.

To characterize the interstitial space in rat brain cortex under normal conditions and during arrest of blood supply, Lundbaek and Hansen [9] used a microelectrode method. It appears that two characteristics, the interstitial volume fraction ε and the tortuosity, govern solute transport in the interstitial space. Under control conditions, the interstitial volume fraction was 0.18 ± 0.02 , whereas it decreased to 0.07 ± 0.01 in ischaemia. The tortuosity was 1.40 ± 0.05 in controls and increased to 1.63 ± 0.09 during ischaemia. The measurements demonstrated that arrest of blood supply changes interstitial diffusion characteristics of brain cortex mainly by diminishing the interstitial diffusion space. In a similar experiment [10], the following values were measured respectively: $\varepsilon = 0.20 \pm 0.019$, $T = 1.62 \pm 0.12$. However, for $\varepsilon = 0.05 \pm 0.021$ the tortuosity increased to $T = 2.00 \pm 0.24$. No further changes in ε were found during and up to 120 min after the animal's death. Eventually, tortuosity increased significantly to $T = 2.20 \pm 0.14$.

Using ion-selective microelectrodes, Krizaj et al. [11] determined the extracellular-volume fraction and tortuosity of the cerebellum granular layer, from measurements of ionophoretically induced diffusion profiles of TMA^+ (tetramethylammonium). The measured volume fraction, i.e. porosity, was 0.22 in normal saline, 0.12 in hypotonic medium and 0.60 in hypertonic medium. Tortuosity values were, respectively, 1.70 in the normal saline, 1.79 in the hypotonic medium and 1.50 in the hypertonic medium. A similar range of the average brain tortuosity was reported in numerous studies and reviews [1,4,12–17].

It should be underlined that the structure of the ECS, in spinal cord especially, gives rise to spatial anisotropy [18]. Rice et al. [12] measured extracellular diffusion properties in three orthogonal axes of the molecular and granular layers of isolated turtle cerebellum with the use of iontophoresis of TMA^+ . Diffusion in the ECS of the molecular layer is known to be anisotropic. The x - and y -axes are in the plane parallel to the pial surface of this lissencephalic cerebellum with the x -axis in the direction of the parallel fibres. The z -axis is perpendicular to this plane. The average tortuosity values obtained were $T_x = 1.44$, $T_y = 1.95$ and $T_z = 1.58$. In turn,

the granular layer was isotropic with a single tortuosity value of 1.77. The molecular layer had $\varepsilon = 0.31 \pm 0.01$, whereas in the granular layer $\varepsilon = 0.22 \pm 0.01$. The schematic anisotropic structure of the ECS is shown, for instance, in [19].

Diffusion and tortuosity in the isolated rat spinal cord were investigated by Prokopova et al. [20]. Diffusion in grey matter remained isotropic ($T = 1.65$), whereas in white matter it became anisotropic, i.e. diffusion is easier along the fibres ($T = 1.38$) than across the fibres ($T = 1.80$). Further measurements confirmed the tortuosity anisotropy in the rat brain to be in the range of 1.46–1.72 [21,22].

Assaf and Cohen [23] used magnetic-resonance images to compute *in vitro* water displacement in rat spinal cord [24]. They found that changes in the diffusion characteristics of white matter upon maturation are responsible for the emergence of grey/white matter contrast. Brain extracellular tortuosity in different conditions was investigated in the work of Pfeuffer et al. [25]. A wide range of tortuosity and porosity values was found after cardiac arrest.

All the above-mentioned results point out that the tortuosity/porosity interplay in ECS under various external conditions must be carefully analysed. This was the aim of the present work.

Diffusion of molecules of different molecular mass

The substantial changes observed in the diffusion parameters could affect the diffusion and aggravate the accumulation of ions, neurotransmitters, metabolic substances and drugs used in therapy of nervous diseases and thus contribute to ischaemic central-nervous-system damage [10]. The diffusion properties of TMA^+ , a relatively small ion with an apparent molecular mass of 75 Da, can be compared particularly with those of biologically important ions and neurotransmitters. However, the diffusion parameters of substances with greater molecular mass, such as glucose (180 Da), ATP (500 Da), various neurohormones and neuropeptides (e.g. dynorphin, substance P, galanin, which are 1000–3000 Da) and nerve growth factor ($\approx 40\,000$ Da), could be altered in both 'early' and 'late' stages of ischaemia.

It was found that dextran molecules of 3 or 10 kDa diffuse in the rat cortex the same way as TMA^+ , whereas 40 and 70 kDa dextrans diffuse significantly more slowly [26]. The diffusion coefficient of dextran in agarose gel, D_g , and the apparent diffusion coefficient, D_e , in brain tissue were determined. Values of the tortuosity, $T = (D_g/D_e)^{1/2}$, for the 3 and 10 kDa dextrans were 1.70 and 1.63, respectively, which were consistent with previous values derived from TMA^+ measurements in cortex. Tortuosities for the 40 and 70 kDa dextrans are significantly larger, with values of 2.16 and 2.25, respectively. This suggests that the ECS may have local constrictions that hinder the diffusion of molecules above a critical size that matches the size range of many neurotrophic compounds. As was pointed out by Nicholson

and Syková [1], there is increasing evidence of selective 'filtering' of large molecules that might exclude them from certain regions of the ECS.

Tao and Nicholson [27] measured the effective diffusion coefficient in rat cortical slices and compared it with the diffusion coefficient in gel, D_g , for three negatively charged proteins, lactalbumin (14.5 kDa), ovalbumin (45 kDa) and BSA (66 kDa). From these data the tortuosity, $T = (D_g/D_e)^{1/2}$, was calculated, with a value of 2.24 for lactalbumin, 2.50 for ovalbumin and 2.26 for BSA. The results show that proteins as large as BSA may diffuse through brain ECS, but their diffusion is more hindered than smaller molecules such as TMA⁺ or penicillin, for which $T = 1.62$ [28].

To understand what factors contribute to the overall tortuosity, experimental measurements of the diffusion of neuroactive molecules in brain tissue were made [14]. Results show that substances confined to the ECS diffuse more slowly than in free solution for two reasons [29]. On the one hand, cellular obstacles increase the pathlength that molecules need to travel; this is the conventional interpretation of tortuosity, normally known as geometrical tortuosity. On the other hand, viscous interactions with extracellular macromolecules and stationary cell walls also slow down diffusion. Both geometric and viscous components of tortuosity determine the overall value of T .

Thus far it has not been clear what component of tortuosity may be allocated to cellular obstacles and what component represents the interactions with the extracellular medium ('geometric' and 'viscous' tortuosity respectively). The work of Rusakov and Kullmann [14] provided some numerical simulations of ECS diffusion. It seems that for molecules with a size comparable with the extracellular cleft, the predominant effect is the viscous drag of cell walls. For small diffusing particles, in contrast, the macromolecular obstacles in the ECS retard diffusion. The main parameters relating the diffusion coefficient within the extracellular medium to the one in free solution are the intercellular gap width and the volume fraction occupied by macromolecules. The upper limit of tortuosity for small molecules predicted by this theory is around 2.2 (implying a diffusion coefficient approximately five times lower than the bulk diffusion found in free medium).

In the work of Rusakov and Kullmann [14], experimental data were fitted with the help of the 'adjustable' parameter N , representing the volume fraction occupied by large extracellular macromolecules. However, the resulting fitting functions in that work are not well adjusted to experimental data. An alternative would be to relate the 'viscous' part of the tortuosity, used in [14], with the conventional complex parameter in hindered diffusion models [30,31].

According to the approach described in [32,33], an overall tortuosity can be obtained by the combination of

the two tortuosity types and is formulated as:

$$T = T_g T_v = (D_0/D_e)^{1/2} \quad (1)$$

where T_g is the 'geometrical' part of overall tortuosity, T , and T_v is the 'viscous' part of the tortuosity.

Since the viscous component of tortuosity is difficult to characterize, it is better to use the hindered diffusion approach, as we shall discuss below.

Hindered diffusion

As we mentioned above, it is necessary to separate the geometrical tortuosity, which is usually constant (or fixed) for some given conditions, from other effects arising during diffusion [7,34], when the ratio $(D_0/D_e)^{1/2}$ is used for diffusion analysis. Usually, besides geometrical tortuosity, another tortuosity term is added, named viscous tortuosity. As we shall see, the hindered diffusion concept is well adapted to explain the differences in diffusion encountered in several real situations, such as in ECS diffusion [30,35].

Two kinds of approach may be used to describe hindered diffusion. The first one [36,37] is used when we consider diffusion in porous media on a microscopic scale, which may be represented by the equation:

$$D_e = D_0 (\varepsilon/T_g^2) F_1(\lambda) F_2(\lambda) \quad (2)$$

where $\lambda = a_e/r_0$, in which a_e is the Einstein radius of the diffusing molecule and r_0 is the pore radius; T_g is the geometrical tortuosity, which is a function of porosity, $T_g = T_g(\varepsilon)$. $F_1(\lambda)$ and $F_2(\lambda)$ are correction factors based on the interaction between solute and solvent molecules with the pore. Function $F_1(\lambda)$ is the steric partition coefficient, which is defined as the cross-sectional area of the pore available to the solute molecule divided by the total cross-sectional area of the pore. It is defined by:

$$F_1(\lambda) = (1 - \lambda)^2 \quad (3)$$

The correction factor $F_2(\lambda)$ accounts for the effect of the pore wall on the solvent properties and is often represented by a series or an exponential function [30,31,36,38,39]. One of the more frequently used relationships is given by Deen [31]:

$$F_2(\lambda) = 1 - 2.1044\lambda + 2.089\lambda^3 - 0.948\lambda^5 \quad (4)$$

The second approach is to consider diffusion in a single pore channel (microscopic scale). Hence $\varepsilon = 1.0$, but often the parameter $1/T_g$ is neglected [35,40], assuming a straight cylindrical pore:

$$D_{ep} = D_0 F_1(\lambda) F_2(\lambda) \quad (5)$$

where D_{ep} is the effective diffusion coefficient in a porous medium channel. When the pore channel is tortuous, the representation of the effective diffusion coefficient must be

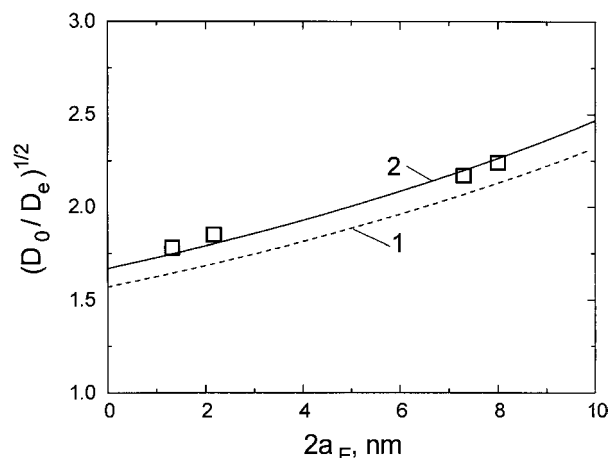


Figure 1 Comparison of experimental data of [14] (□) with the model in eqn (6)

Curve 1, tortuosity $T = 1.57$; curve 2, $T = 1.67$.

corrected to:

$$D_e = D_0 (1/T_g^2) F_1(\lambda) F_2(\lambda) \quad (6)$$

By making the first part of eqn (6) as in eqn (1) we get:

$$(D_0/D_e)^{1/2} = T_g/[F_1(\lambda)F_2(\lambda)]^{1/2} \quad (7)$$

This means that the expression $1/[F_1(\lambda)F_2(\lambda)]^{1/2}$ plays a role similar to the viscous tortuosity, as mentioned in eqn (1).

Nugent and Jain [35] reported that, in membrane pores, linear dextran has a diffusion radius between one-third and one-half of its a_E . Furthermore, for linear random-coil polymers, Deen [31] proposed to use in the hindered-diffusion equation the radius $0.7a_E$. We may thus assume, as a good estimation for the dextran radius, a value of $1/3 a_E$. Let us now analyse the data of Rusakov and Kullmann [14], shown in their paper as Figure 3(A), that represents the dependence of $(D_0/D_e)^{1/2}$ on the size of dextran molecules. Using the geometrical tortuosity calculated by the authors to be $T = 1.571$ and $2r_0 = 20$ nm we have for the model eqn (6), and assuming the validity of eqns (2), (3) and (4), the dependence is shown in Figure 1 (curve 1). Experimental points were borrowed from the original graph presented in [14]. However, the best fit is obtained by curve 2, which corresponds to $T = 1.67$.

The obtained result shows that, by introducing in eqns (2)–(7) the parameters describing the diffusing molecule conformation, it is possible to achieve a better functional description of experimental data without making use of the fitting parameter N . This is important for analysing what molecule shape conformation is better, for example, in drug delivery.

This model was also applied to data on diffusion in tumours of different cell-density arrangement reported in [41].

Effective diffusion coefficients of dextran up to a molecular mass of 2000 kDa ($a_E = 19$ nm) and of liposomes up to 150 nm in diameter were measured in tumours U87 and Mu89 obtained with different cell arrangements: a fast-diffusion group [in CW (cranial window) tumours] and a slow-diffusion group [in DC (dorsal chamber) tumours]. The model described by eqn (1) did not fit the experimental results. In turn, the estimations based on the hindered-diffusion model, eqn (6), give a quite reasonable approach. By using the values of 60–75 nm of interfibrillar half-spacing r_0 , located in the ECS, and model (6), we have for 2000 kDa dextran a diffusion decrease in DC tumours in the order of 0.01–0.03 D_0 , which matches the experimentally measured D_e bounds. The estimation from a micrograph contained in [41] gave, for CW tumours, $r_0 = 200$ –250 nm. Therefore, for liposomes of $a_E = 75$ nm we get a decrease in diffusion to 0.08–0.15 D_0 , which again falls inside the experimentally measured range. These results show the influence of the tortuosity viscous component.

Let us look to what happens with diffusion of small molecules through the brain ECS.

Modelling diffusion of small molecules through the brain ECS

The complexity of the diffusion phenomenon in brain ECS is related with the dynamic brain response to changes in external conditions. In the work of Pfeuffer et al. [25] the brain extracellular tortuosity under different conditions was investigated. A relationship between porosity and tortuosity was used of the form:

$$T = 1/\varepsilon^n \quad (8)$$

The authors found that the tortuosity exponent is variable and depends on the brain tissue behaviour. In healthy neonatal rat brain, $n = 0.31$ in grey matter, whereas $n = 0.46$ in white matter. The exponential index, n , decreases continuously upon induction of global ischaemia and reaches an asymptotic value of around 0.24 (both in grey and white matter) roughly 30 min after ischaemia. It must be underlined that the exponential index for grey matter is lower than in the case of a rigid particle bed packing [32], where usually we have $n = 0.4$ –0.5 [33].

In a recent work several attempts were made to obtain a model for the dependence of T on ε , in particular using Archie's law [42]. On the basis of experimental data in rat neocortex, the authors concluded that T was independent of ε . However, it must be stressed that the Archie equation was obtained many years ago for mineral porous media, which are non-flexible arrangements where the parameter n is constant for a defined porous medium.

The abovementioned data demonstrate the dynamic behaviour of ECS as an interplay of the porosity and tortuosity that is not observed for an inert rigid packing and

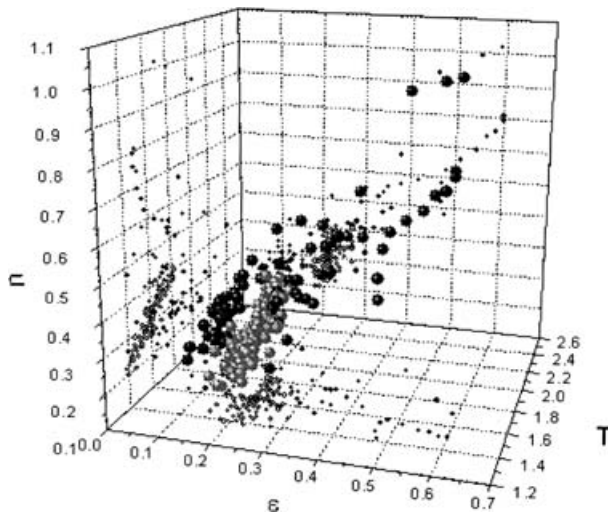


Figure 2 Three-dimensional dependence of the tortuosity index on ε and T

Spheres, three-dimensional data positions: grey spheres, normal ECS conditions; black spheres, abnormal conditions. Small points are projection on axial planes.

is completely different from the one assumed, for example, with Archie's model.

The above results show also that we must pay attention to the dependence of the tortuosity T on ECS volume fraction ε , as well as on the dependence of n on ε (eqn 8). In order to generalize this dependence, we collected data (120 sets) for tortuosity T measured from results on TMA⁺ diffusion and then we calculated the exponential index of eqn (8). Experimental data were gathered from the above-cited articles [14,25–29] as well as from the results mentioned in the papers by Syková and colleagues [43–47]. The small size of TMA⁺ allows us to assume that the obtained tortuosity is in the range of the geometrical value T_g (see Figures 2 and 3).

As may be seen from the graph (Figure 3), the main variation of index n versus porosity concentrates in the range between $n=0.2$ and $n=0.6$ (broken lines). Furthermore, most of the exponential index values stay between two border lines encompassing the vast majority of the experimental points. The upper border line is given by the expression:

$$n = 0.26 + 0.3\varepsilon + \varepsilon^2 \quad (9)$$

and the lower border line is given by:

$$n = 0.2 + \varepsilon^2 \quad (10)$$

The upper border line defined by eqn (9) may be related to 'topologically' dense cell arrangement, whereas the lower (eqn 10) is related to loose arrangement. Scattering of n in the neighbourhood of $\varepsilon = 0.3$ is discussed below. Border

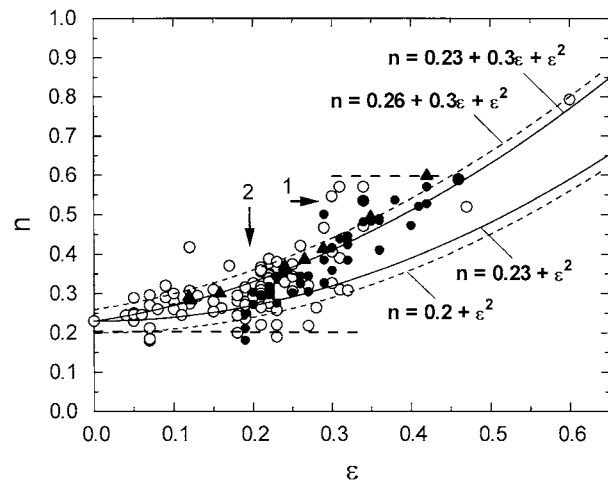


Figure 3 Dependence of n on porosity (ECS volume fraction) calculated from the experimental data of TMA⁺ diffusion gathered from published articles

Broken straight lines correspond to the main range of n , and broken curves are boundary eqns (9) and (10). Continuous curves, eqns (11) and (12). ●, Data [43] for rat neocortex and subcortical white matter during postnatal development and [45] for foetal grafts young and old (where curves 1 and 2 represent young and mature brain respectively). ○, Experimental data gathered from [14,25–29] as well as from the results of Syková and colleagues [42,46,47]. ▲, Osmotic changes in rat neocortex [42].

lines given by eqns (9) and (10) may both be obtained from the equation:

$$n = n_0 + a\varepsilon + \varepsilon^2$$

where n_0 corresponds to extrapolation for $\varepsilon = 0$, and $a = 0.3$. If we extrapolate eqns (9) and (10) for $\varepsilon = 0$, we obtain as an average value $n_0 = 0.23$. We then have the corrected equations:

$$n = 0.23 + 0.3\varepsilon + \varepsilon^2 \quad (11)$$

$$n = 0.23 + \varepsilon^2 \quad (12)$$

which contracts slightly the region of the tortuosity index variation, increasing the number of outliers. Nevertheless, it presents the advantage of equalizing the boundary conditions for $\varepsilon = 0$.

The model validity was checked with experimental data on TMA⁺ ion diffusion in two different kinds of brain tissue, rat cortex and turtle cerebellum, obtained from the work of Rusakov and Kullmann [14]. We have two data sets of different types: the one obtained from rat cortex is a topologically loose cell arrangement, whereas turtle cerebellum presents a dense arrangement. Original experimental data of [14] together with the previously obtained modelling curves are shown in Figure 4, where curves 1 and 2 represent models in eqns (13) and (14). Thus, for a topologically dense arrangement (turtle cerebellum), we have:

$$T = 1/\varepsilon^{0.23+0.3\varepsilon+\varepsilon^2} \quad (13)$$

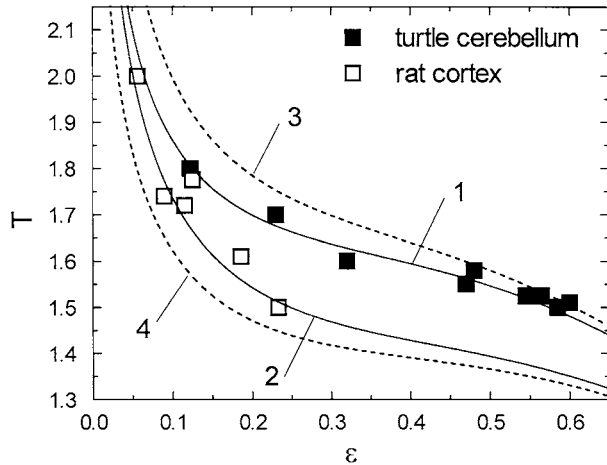


Figure 4 Dependence of tortuosity T on volume fraction ε of ECS

Data from [14] are shown: ■, turtle cerebellum; □, rat cortex. Curves 1 and 2, eqn (13) and (14), respectively; curves 3 and 4, eqn (8) when n is defined by eqns (9) and (10), respectively.

whereas, for a loose arrangement (rat cortex) we have:

$$T = 1/\varepsilon^{0.23+\alpha^2} \tag{14}$$

Curves 3 and 4 in Figure 4 correspond to eqn (8) when n is defined by eqns (9) and (10) respectively.

As may be seen, boundary curves 3 and 4 enclose the experimental data well. The proposed fitting functions correlate with experimental data and provide a simple and reasonable explanation for the observed variation in tortuosity versus porosity.

Now we can go back to the data presented in Figure 3. On the basis of the boundary limits for $n = 0.2$ and 0.6 , shown in Figure 3 as broken lines, it is possible to obtain a probable range of the tortuosity variation drawn in Figure 5. If we consider the tortuosity as $T = (D_0/D_e)^{1/2}$ an important conclusion may be drawn: as compared with an inert granular bed packing, where $T = 1/\varepsilon^{1/2}$ (Figure 5, curve 7) [33], the tortuosity variation for ECS is less abrupt. This means that, when the ECS fraction ε decreases, cellular structure (presumably the cell membrane) rearranges the void space in order to keep the diffusion within an acceptable range. Therefore, this autocorrection phenomenon gives the living tissue the ability to support diffusion at a level 2-fold higher (or more) than in an inert granular bed packing.

Moreover, even with a drastic ECS decrease, the cellular system is still able to maintain diffusivity between certain bounds by decreasing tortuosity. To explain physically the tortuosity jump at about $\varepsilon = 0.3$ (see Figures 3 and 5), further investigation will be needed. Nevertheless, on the basis of experimental data available [2,10,25,44,46,48] it is possible to speculate that the tortuosity jump might be related to some pathological states (X-irradiation, encephalomyelitis, etc.).

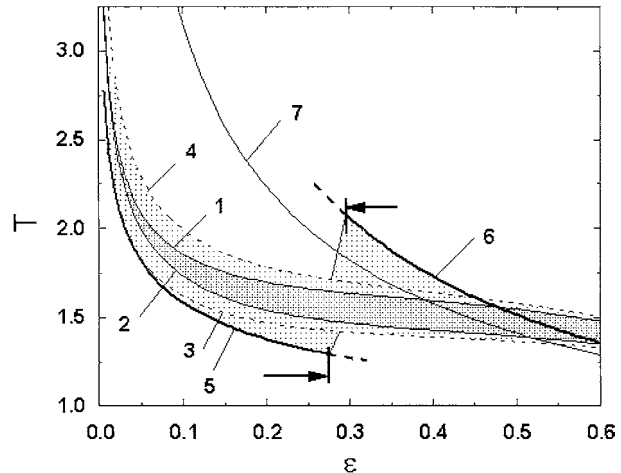


Figure 5 Range of ECS tortuosity, determined from diffusion data of TMA^+ , for different void fractions of the brain ECS (light shaded area)

Curves 1 and 2, functions (13) and (14); curves 3 and 4, eqn (8) when n defined by eqns (9) and (10); curves 5 and 6, lower $T = 1/\varepsilon^{0.2}$ and upper $T = 1/\varepsilon^{0.6}$ levels; curve 7, conventional dependence of the tortuosity for granular bed $T = 1/\varepsilon^{0.5}$.

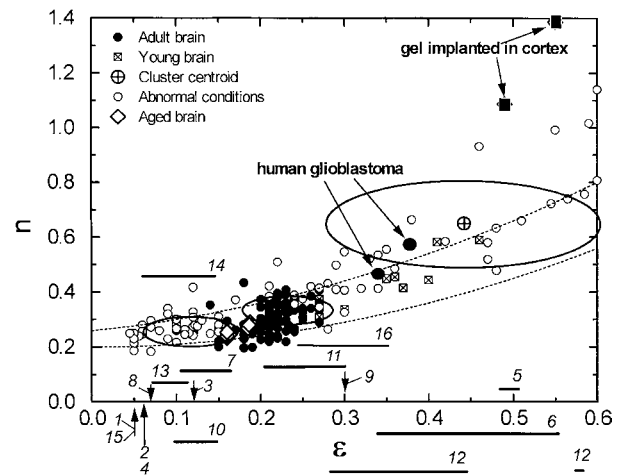


Figure 6 Representation of normal and abnormal brain tissue distribution

n versus ε : 1, anoxia; 2, blood pressure 30 mmHg; 3, blood pressure 40 mmHg; 4, 10 min after death; 5, X-irradiation acute state; 6, X-irradiation chronic state; 7, hypoxia; 8, terminal apoxia; 9, recovery after anoxia; 10, hypertermia; 11, astrogliosis-stab wounds; 12, experimental autoimmune encephalomyelitis; 13, implication of 50 mM K^+ ; 14, ischaemia; 15, 80 mM K^+ ; 16, cortical grafts.

We investigated this issue with the help of cluster analysis. Clustering is normally used to classify observations into groups whenever these groups are not yet identified. The obtained results show that the data set can be divided into three clusters, separating data corresponding to normal brain behaviour from two clusters corresponding to abnormal brain behaviour (Figure 6). Normal and

abnormal brain conditions defined in terms of n versus ε are shown in Figure 6.

During maturation ECS brain volume changes significantly. According to [2], neonatal rat brain has ε between 0.36 and 0.46 and $T \approx 1.5$, whereas the healthy brain of an adult rat has ε between 0.19 and 0.22 and $T \approx 1.6$. In the case of ischaemia the porosity decreases to $\varepsilon = 0.05 \pm 0.021$, and tortuosity increases to $T \approx 2.00$ [10]. No further changes in ε were found during and up to 120 min after the animal's death, but tortuosity increased significantly to $T = 2.20 \pm 0.14$. Post-mortem brain is no longer able to control the diffusion process.

The transition from neonates to mature brain corresponds to a significant change in ε and crosses the region of the tortuosity jump but, as pointed out in [2], the tortuosity variation in a healthy brain is not statistically significant at any age. Tortuosity in this case falls between curves 1 and 2 (Figure 5). However, young brain tortuosity is closer to the upper borderline (Figure 5, curve 1), whereas aged brain tortuosity tends to be closer to the lower borderline (Figure 5, curve 2) [3,46]. The observed changes in ECS diffusion parameters during aging may contribute to functional deficits and memory loss [3].

Index n may be useful for the characterization of the anomalous brain tissue. As an example we shall consider a neural tissue formation within porous hydrogels implanted in brain and spinal cord lesions [47]. This issue was investigated as a potential method to repair tissue defects in the central nervous system by replacing lost tissue and by promoting the formation of a histotypic tissue matrix that could facilitate and support regenerative axonal growth. The following values were obtained for implanted and non-implanted hydrogels: implanted hydrogels, porosity $\varepsilon \approx 0.49$ and tortuosity $T \approx 2.17$ corresponding to $n = 1.09$; non-implanted hydrogels, $\varepsilon \approx 0.8$ and $T \approx 1.13$ corresponding to $n = 0.5$. As we may see in Figure 6, in any case the index n is rather distant from any of the previously identified clusters.

According to Figure 3, for ε around 0.49 the expected index n must be in the range of 0.5–0.6. Moreover, at $\varepsilon = 0.49$ the tissue tortuosity is close to the inert granular packing tortuosity (Figure 5). The tortuosity generated by cells presence may be estimated as $T_c = 1/\varepsilon^{1/2} = 1.43$. The experimental values obtained for tortuosity, 2.17 and 1.13, mean that gel matrix, and not growing tissue, is mainly responsible for the overall tortuosity, since these results match those obtained for diffusion in gel-matrix-type porous media [33].

Let us use another example. Research of Syková et al. [45] was devoted to measuring ECS diffusion parameters in host cortex, host corpus callosum, fetal cortical tissue transplanted into host midbrain (81–135-day-old 'young' C-grafts and 336–351-day-old 'old' C-grafts), foetal tectal tissue transplanted into host midbrain (105–150-day-old T-grafts)

and fetal cortical tissue transplanted to host cortex (209–245-day-old C-C-grafts). Calculated indexes are shown in Figure 3. For young grafts, indexes are on the top of the 'jump' region (marked as 1) that points out to abnormal tissue behaviour. For old grafts the indexes (marked as 2) lie in the region corresponding to normal brain behaviour and are an evidence of the observed well-incorporated grafts.

The main advantage of the use of the tortuosity index is that it may be easily adopted for recalculation of tortuosity or porosity if one of these parameters is already known. By rearranging eqn (8) we have $T\varepsilon^n = 1$ and

$$\ln T + n \ln \varepsilon = 0 \quad \text{or} \quad n = -\ln T / \ln \varepsilon \quad (15)$$

Tortuosity and porosity representation in the logarithmic form (eqn 15) may be a promising tool for further implementation of an approach based on the theory of information [49]. Live tissue reacts differently under different environmental conditions [50]. In some pathophysiological states, ε and T behave as independent variables. A persistent increase in T (without a decrease in ε) is always found during astrogliosis and in myelinated tissue, suggesting that glial cells can act as diffusion barriers, making the nervous tissue less permeable and thereby playing an important role in signal transmission, in tissue regeneration and in pathological states [17,18]. These changes are important in understanding some diseases [3]. In particular, during aging, the movement of substances is retarded in the narrower clefts. This is partly compensated for by a decrease in the diffusion barriers that may be formed by macromolecules of the extracellular matrix. Hence, diffusion in ECS must be considered together with macromolecules of the extracellular matrix for explanation of the diffusion phenomenon diversity [4,14,16,51]. It is why we shall analyse now what happens with the diffusion of macromolecules.

Discussion: the diversity of diffusion mechanisms in brain

As we have seen, diffusion in ECS may significantly change according to brain condition, thereby giving rise to different diffusion parameter values. Furthermore, diffusion will also depend on the molecular mass, on the concentration and on the shape of the macromolecule. The polymer concentration increase in regions with diffusion stagnation may totally exclude from these regions some of the diffusing molecules and therefore decrease the pathway tortuosity. On the other hand, increasing the average polymer concentration will increase, as we have seen above, hindered diffusion.

The effect of large molecules in sufficient concentration on diffusion of TMA⁺ in ECS is illustrated in [17]. Superfusion

through a slice of spinal cord with a solution containing either 40 or 70 kDa dextran (concentration in solution 1 or 2%) or 0.1% hyaluronic acid (1600 kDa) results in a significant increase in tortuosity; $T = 1.72$ – 1.77 for dextran and $T = 2$ for hyaluronic acid, whereas in standard physiological solution $T = 1.57$. Variation of ECS ε was limited to about 10%.

An example of tortuosity reduction by increasing stagnant diffusion regions with the consequent 'smoothing' pathway tortuosity is seen in the work of Hrabetova and Nicholson [52], where the effect of dextran on the diffusion in a thick-slice ischaemia model was studied. This study shows that the tortuosity in thick slices from rat neocortex may increase or decrease depending on experimental conditions, whereas ECS volume fraction remains constant and reduced to $\varepsilon = 0.1$. Using TMA^+ diffusion, the authors found that, for ischaemia, tortuosity rose from a value of 1.66 to 1.99 in thick slices as expected. However, the tortuosity dropped to 1.54 when 70 kDa dextran was added to the bathing medium. This apparent contradictory effect might be explained by the excessively low porosity of the ischaemic tissue, which might have been increased by a swelling effect due to the presence of dextran.

The effect of the macromolecule shape on diffusion is illustrated in the work of Zoli et al. [19]. The authors reported that even polymers with a molecular mass of about 1000 kDa can diffuse in the ECS as long as they have an appropriate elongated shape.

The diffusion properties of two types of large co-polymer of HPMA [N-(2-hydroxypropyl)methacrylamide], developed as water-soluble anti-cancer drug carriers, was discussed by Syková et al. [17]. In a study carried out in rat cortical slices the authors used linear HPMA polymeric chains of 1000 kDa and star-like systems, containing either albumin (179 kDa) or IgG (319 kDa) in the centre with HPMA side branches. Long-chain HPMA polymers diffuse through the ECS with the same tortuosity as small molecules such as TMA^+ . However, when the HPMA is shaped into a more bulky globular molecule with the help of a graft co-polymer the tortuosity increases to about 2.3. Tortuosity for long-chain HPMA was always found to be smaller than tortuosity of globular co-polymers. These data show that the shape of the substance is a limiting factor in its movement through the ECS. In a further research, Prokopova-Kubinová et al. [53] conjugated HPMA with BSA to obtain a bulky polymer of 176 kDa molecular mass. As a consequence, the tortuosity rose to 2.27, a value similar to the one previously obtained with BSA alone and with 70 kDa dextran. The reason for the observed differences may be explained by the changes in molecular shape.

Graphical representation of the tortuosity versus molecular mass taken from the aforementioned articles is shown in Figure 7. As may be seen, one of the main

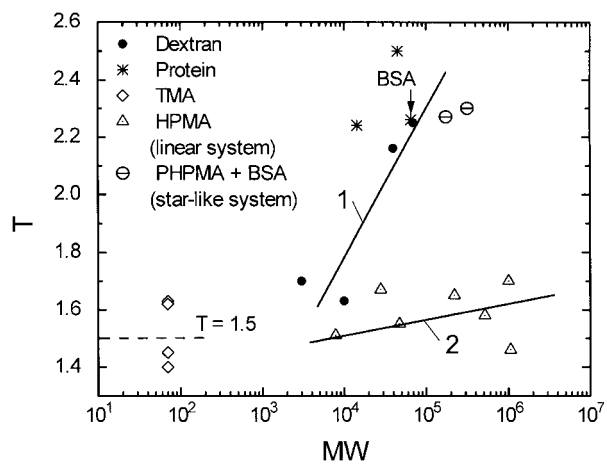


Figure 7 Tortuosity versus molecular mass (MW) as defined in ECS diffusion experiments

Curve 1, tortuosity trend for pure molecules and star-like systems; curve 2, linear HPMA co-polymers tortuosity trend. PHPMA, poly[N-(2-hydroxypropyl)methacrylamide] [53].

characteristics affecting diffusion in ECS is supposed to be the macromolecule's shape rather than the molecular mass.

Relatively rigid globular particles such as the proteins presented in Figure 7 withstand hindered diffusion and therefore show higher total tortuosity if the tortuosity is calculated as $T = (D_0/D_e)^{1/2}$.

Dextran and other polysaccharides contain a backbone of D-glucose units [54] and are characterized by a relatively open-chain (randomly coiled) molecular structure [55]. For a linear, random-coil polymer, Deen [31] suggested the use in the hindered diffusion equation of a radius $\approx 0.7a_e$. Also, Nugent and Jain [35] reported that, in membrane pores, linear dextran has a diffusion radius around one-third to one-half of its a_e . Therefore a lower tortuosity $T = (D_0/D_e)^{1/2}$ should be expected. However, the elongated shape of the dextran molecules gives them a behaviour similar to that observed for globular proteins.

Tortuosity for BSA co-polymer with a star-like structure is close to globular proteins, owing to similar molecular mass and shape.

The molecular size of HPMA was not defined in [17,53], but it is possible to estimate it by using the information available on polyacrylamide. Polyacrylamide exhibits a flexible spherical shape between 15 and 30 °C [56,57]. For the solutions of polyacrylamide the relaxation time is about 0.8–1.16 ms, but the molecular size is significantly higher than dextran (for dextran of 70 kDa, $a_e = 11$ nm [58]): 320 kDa, size 40 nm; 920 kDa, size 98 nm and 2900 kDa, size 206 nm [59]. If molecular exclusion and a pathway-'smoothing' effect are taken into account then these macromolecules will be able to diffuse in a limited volume of

ECS through the large size. This means that parts of the intercellular structures may act as molecular sieves. This speculation seems important, as the type of macromolecules mentioned are considered as water-soluble anti-cancer drug carriers. As a tumour has a larger ECS volume than normal brain tissue, macromolecules of the appropriate size would be able to penetrate only into the tumour tissue, thereby avoiding negative chemotherapeutic effects on normal brain cells.

In conclusion, we may say that, with the help of the approach proposed in the present study, it is possible in the first place to characterize ε and T for a defined pathological case. Each pathological state may be characterized by a specific set of parameters, and the tortuosity index, n , introduced in the form of a logarithmic ratio between T and ε , is correlated with several pathological situations. We found that upon different external conditions, for instance, oxygen depletion, the ECS porosity decreases and cells (presumably through membrane rearrangements) adjust the void space to keep the diffusion within a defined range, which gives the living tissue the ability to support diffusivity up to 2-fold or more times the values found in conventional granular bed packing. Thus even with a dramatic ECS decrease, the cellular system is still able to sustain a given diffusion by reducing T .

Our research showed also that the hindered diffusion model is the most suitable for the description of macromolecular diffusion in brain ECS. The hindered diffusion is affected by three factors: molecular mass, concentration and molecule shape of the diffusing macromolecule.

The present approach allows us to define the mechanisms that affect macromolecular motion in ECS and thereby enables us to select the best-fitted transport macromolecule for drug delivery or to elaborate a suitable strategy to combat brain diseases. This might be important in brain clinical treatment.

Finally, obtained results show that living tissues have the unique possibility of controlling mass-transfer processes by adjusting ECS configuration by porosity and tortuosity that can be described by a three-parametric model. This situation does not occur in inert materials, for which the dependence of the porosity on tortuosity may be defined by two parameters. The developed three-parametric model enabled us to define a domain where the vast majority of the experimental points are enclosed.

Acknowledgments

We thank Fundação para a Ciência e Tecnologia (FCT) for the grant accorded to A.Y. and for the project POCTI/37500/EQU/2001, which provided the means for the present research. This project is partially funded by FEDER (Fonds

Européen de Développement Régional). We also wish to mention the support from the Gulbenkian Foundation that funded a grant for M.M.

References

- Nicholson, C. and Syková, E. (1998) *Trends Neurosci.* **21**, 207–215
- Syková, E. (1997) *Neuroscientist* **3**, 28–41
- Syková, E., Mazel, T. and Simonová, Z. (1998) *Exp. Gerontol.* **33**, 837–851
- Syková, E. and Chvatal, A. (2000) *Neurochem. Int.* **36**, 397–409
- Satterfield, C. N. (1970) *Mass Transfer in Heterogeneous Catalysis*, M.I.T. Press, Cambridge, MA
- Bear, J. (1972) *Dynamics of Fluids in Porous Media*, Dover Publications, New York
- Mota, M., Teixeira, J. A. and Yelshin, A. (1999) *Separation Purif. Technol.* **15**, 59–68
- Nicholson, C. and Rice, M. E. (1987) *Can. J. Physiol. Pharmacol.* **65**, 1086–1091
- Lundbaek, J. A. and Hansen, A. J. (1992) *Acta Physiol. Scand.* **146**, 473–484
- Syková, E., Svoboda, J., Polak, J. and Chvatal, A. (1994) *J. Cereb. Blood Flow Metab.* **14**, 301–311
- Krizaj, D., Rice, M. E., Wardle, R. A. and Nicholson, C. (1996) *J. Physiol. (London)* **492**, 887–896
- Rice, M. E., Okada, Y. C. and Nicholson, C. (1993) *J. Neurophysiol.* **70**, 2035–2044
- van der Toorn, A., Syková, E., Dijkhuizen, R. M., Vorisek, I., Vargova, L., Skobisova, E., Campagne, M. V. L., Reese, T. and Nicolay, K. (1996) *Magn. Reson. Med.* **36**, 52–60
- Rusakov, D. A. and Kullmann, D. M. (1998) *Proc. Natl. Acad. Sci. U.S.A.* **95**, 8975–8980
- Egelman, D. M. and Montague, P. R. (1999) *Biophys. J.* **76**, 1856–1867
- Chen, K. C. and Nicholson, C. (2000) *Proc. Natl. Acad. Sci. U.S.A.* **97**, 8306–8311
- Syková, E., Mazel, T., Vargová, L., Vorisek, I. and Prokopova-Kubinová, S. (2000) *Prog. Brain Res.* **125**, 155–178
- Prokopova-Kubinová, S. and Syková, E. (2000) *J. Neurosci. Res.* **62**, 530–538
- Zoli, M., Jansson, A., Syková, E., Agnati, L. F. and Fuxe, K. (1999) *Trends Pharmacol. Sci.* **20**, 142–150
- Prokopova, S., Vargova, L. and Syková, E. (1997) *Neuroreport* **8**, 3527–3532
- Vorisek, I. and Syková, E. (1997) *J. Neurophysiol.* **78**, 912–919
- Chvátal, A., Berger, T., Vorisek, I., Orkand, R. K., Kettenmann, H. and Syková, E. (1997) *J. Neurosci. Res.* **49**, 98–106
- Assaf, Y. and Cohen, Y. (2000) *Magn. Reson. Med.* **43**, 191–199
- Assaf, Y., Mayk, A. and Cohen, Y. (2000) *Magn. Reson. Med.* **44**, 713–722

- 25 Pfeuffer, J., Dreher, W., Syková, E. and Leibfritz, D. (1998) *Magn. Reson. Imaging* **16**, 1023–1032
- 26 Nicholson, C. and Tao, L. (1993) *Biophys. J.* **65**, 2277–2290
- 27 Tao, L. and Nicholson, C. (1996) *Neuroscience* **75**, 839–847
- 28 Lehmenkuhler, A., Kersting, U. and Nicholson, C. (1988) *Brain Res.* **444**, 181–183
- 29 Rusakov, D. A. and Kullmann, D. M. (1998) *Trends Neurosci.* **21**, 469–470
- 30 Suzuki, M. (1990) *Adsorption Engineering*, Kodansha-Elsevier, Tokyo
- 31 Deen, W. M. (1987) *Am. Inst. Chem. Eng. J.* **33**, 1409–1425
- 32 Mota, M., Teixeira, J. A., Bowen, R. and Yelshin, A. (2000) in *Proceedings of 8th World Filtration Congress*, 3–7 April (2000), pp. 57–60, Filtration Society, Brighton, U.K.
- 33 Mota, M., Teixeira, J. A. and Yelshin, A. (2001) *Biotechnol. Prog.* **17**, 860–865
- 34 Mota, M., Teixeira, J. A. and Yelshin, A. (1998) in *Proceedings of 2nd European Symposium on Biochemical Engineering Science*, Porto, 16–19 September 1998 (Feyo de Azevedo, Ferreira, E., Luben, K. and Osseweijer, P., eds.), pp. 93–98, University of Porto, Porto
- 35 Nugent, L. J. and Jain, R. K. (1983) *Am. Inst. Chem. Eng. J. Symp. Ser.* **79**, 1–10
- 36 Limbach, K. W. and Wei, J. (1990) *Am. Inst. Chem. Eng. J.* **36**, 242–248
- 37 Blanch, H. W. and Clark, D. S. (1996) *Biochemical Engineering*, Marcel Dekker, New York
- 38 Baltus, R. E. and Anderson, J. L. (1983) *Chem. Eng. Sci.* **38**, 1959–1969
- 39 Anderson, J. L., Kathawalla, I. A. and Lindsey, J. S. (1988) *Am. Inst. Chem. Eng. J. Symp. Ser.* **84**, 35–39
- 40 Netrabukkana, R., Lourvanij, K. and Rorrer, G. L. (1996) *Ind. Eng. Chem. Res.* **35**, 458–464
- 41 Pluen, A., Boucher, Y., Ramanujan, S., McKee, T. D., Gohongi, T., di Tomaso, E., Brown, E. B., Izumi, Y., Campbell, R. B. et al. (2001) *Proc. Natl. Acad. Sci. U.S.A.* **98**, 4628–4633
- 42 Kume-Kick, J., Mazel, T., Vorisek, I., Hrabetová, S., Tao, L. and Nicholson, C. (2002) *J. Physiol. (London)* **542**, 515–527
- 43 Lehmenkuhler, A., Syková, E., Svoboda, J., Zilles, K. and Nicholson, C. (1993) *Neuroscience* **55**, 339–351
- 44 Roitbak, T. and Syková, E. (1999) *Glia* **28**, 40–48
- 45 Syková, E., Roitbak, T., Mazel, T., Simonová, Z. and Harvey, A. R. (1999) *Neuroscience* **91**, 783–798
- 46 Syková, E., Vargova, L., Prokopova, S. and Simonová, Z. (1999) *Glia* **25**, 56–70
- 47 Woerly, S., Petrov, P., Syková, E., Roitbak, T., Simonová, Z. and Harvey, A. R. (1999) *Tissue Eng.* **5**, 467–488
- 48 Norris, D. G. (2001) *NMR Biomed.* **14**, 77–93
- 49 Yelshin, A. (1996) *J. Membrane Sci.* **117**, 279–289
- 50 Jansson, A., Mazel, T., Andbjør, B., Rosé, L., Guidolin, D., Zoli, M., Syková, E., Agnati, L. F. and Fuxe, K. (1999) *Neuroscience* **91**, 69–80
- 51 Netti, P. A., Berk, D. A., Swartz, M. A., Grodzinsky, A. J. and Jain, R. K. (2000) *Cancer Res.* **60**, 2497–2503
- 52 Hrabetova, S. and Nicholson, C. (2000) *J. Cereb. Blood Flow Metab.* **20**, 1306–1310
- 53 Prokopova-Kubinová, S., Vargová, L., Tao, L., Ulbrich, K., Syková, E. and Nicholson, C. (2001) *Biophys. J.* **80**, 542–548
- 54 Budavari, S. (ed.) (1989) *The Merck Index, An Encyclopedia of Chemicals, Drugs, and Biologicals*, Merck and Co., Rahway, NJ
- 55 Laurent, T. C. and Granath, K. A. (1967) *Biochim. Biophys. Acta* **136**, 191–198
- 56 Jones, W. M. (1976) *J. Phys. D Appl. Phys.* **9**, 721–733
- 57 Jones, W. M. (1979) *J. Phys. D Appl. Phys.* **12**, 369–382
- 58 Davidson, M. G. and Deen, W. M. (1988) *Macromolecules* **21**, 3474–3481
- 59 Gramain, Ph. and Myard, Ph. (1981) *Macromolecules* **14**, 180–184

Received 8 August 2003/29 September 2003; accepted 10 October 2003
Published as Immediate Publication 10 October 2003, DOI 10.1042/BA20030140
